

# Relic density and PAMELA events in a heavy wino dark matter model with Sommerfeld effect

Subhendra Mohanty <sup>a</sup>, Soumya Rao <sup>a</sup> and D.P.Roy <sup>b</sup>

<sup>a</sup>*Physical Research Laboratory,  
Ahmedabad 380009, India.*

<sup>b</sup>*Homi Bhabha Centre for Science Education,  
Tata Institute of Fundamental Research,  
Mumbai-400088, India.*

## Abstract

In a wino LSP scenario the annihilation cross section of winos gravitationally bound in galaxies can be boosted by a Sommerfeld enhancement factor which arises due to the ladder of exchanged  $W$  bosons between the initial states. The boost factor obtained can be in the range  $S \simeq 10^4$  if the mass is close to the resonance value of  $M \simeq 4$  TeV. In this paper we show that if one takes into account the Sommerfeld enhancement in the relic abundance calculation then the correct relic density is obtained for 4 TeV wino mass due to the enhanced annihilation after their kinetic decoupling. At the same time the Sommerfeld enhancement in the  $\chi\chi \rightarrow W^+W^-$  annihilation channel is sufficient to explain the positron flux seen in PAMELA data without significantly exceeding the observed antiproton signal. We also show that  $(e^- + e^+)$  and gamma ray signals are broadly compatible with the Fermi-LAT observations. In conclusion we show that a 4 TeV wino DM can explain the positron and antiproton fluxes observed by PAMELA and at the same time give a thermal relic abundance of CDM consistent with WMAP observations.

## 1. INTRODUCTION

There is a great deal of activity in recent years in trying to interpret the excess of hard positron events reported by the PAMELA experiment [1] as a possible signal for dark matter [2]. In the framework of the minimal supersymmetric standard models (MSSM), one expects the wino to be the lightest supersymmetric particle, and hence a dark matter candidate, in the anomaly mediated supersymmetry breaking model [3–6] as well as some string inspired models [7, 8]. More over, such a wino dark matter is known to give the right cosmological relic density for a relatively heavy wino mass of  $\sim 2$  TeV [9]. It is also widely recognized that such a heavy wino dark matter can naturally account for a hard positron signal from their pair-annihilation into the  $W^+W^-$  channel, followed by the leptonic decay of the W bosons [10–13]. It is equally well known, however, that the model would need a very large boost factor to match the observed magnitude of the positron signal.

One of the main theoretical mechanisms invoked to explain the above mentioned boost factor is the so called Sommerfeld effect [13–18]. It is recognized, however, that in order to get a large enhancement of DM annihilation cross-section (boost factor), the DM mass has to lie very close to one of the Sommerfeld resonances [19–21], in which case the Sommerfeld enhancement will also have a profound effect on the DM relic density. In this work, we shall assume the wino DM mass to lie very close to the first Sommerfeld resonance of about 4 TeV, and see if the Sommerfeld effect can simultaneously account for the right cosmological relic density as well as the large boost factor required to explain the size of the hard positron signal. Recently a quantitative analysis of the Sommerfeld effect in the DM relic density calculation has been made by Feng et al [22, 23] in the context of a new physics scenario, where the effect arises from multiple exchanges of a light gauge boson in a hidden sector. We shall follow their procedure closely for incorporating the Sommerfeld effect in the relic density calculation for a wino DM of the MSSM, where it arises from the multiple exchanges of the standard W boson. We shall see below that for a wino mass of about 4 TeV, the Sommerfeld effect can indeed account for the right WMAP compatible relic density [24] as well as a large boost factor, required to explain the PAMELA positron excess. We shall also see that increasing the wino mass to 4 TeV helps to make the predicted antiproton signal compatible with the PAMELA measurements [25, 26] of  $\bar{p}/p$  ratio by shifting the antiproton peak to higher energies. The flux ratio  $e^+/(e^+ + e^-)$  measured by PAMELA

[1] gets a contribution from the secondary positrons generated by cosmic ray electrons and protons. The measurement of the  $(e^+ + e^-)$  flux by Fermi-LAT [27, 28] along with the measurements of heavier nuclei flux spectrum in the  $(10 - 600)$  GeV range by HEAO-3 [29], ATIC-2 [30] and CREAM [31] fix the parameters of primary cosmic ray background and the diffusion parameters in the galaxy. This leaves us essentially with the boost factor as the free parameter to adjust in comparing the theory with the Pamela positron data. Having fixed the boost factor, which in our case turns out to be  $S = 10^4$ , we show that the  $\gamma$ -rays produced by the DM annihilation do not exceed the diffuse  $\gamma$ -ray observations by Fermi-LAT[32].

The work is organized as follows. In section 2, we summarize the wino DM model along with the procedure for incorporating the Sommerfeld effect in the DM relic density calculation. Then in section 3, we present the results for the DM relic density after incorporating the Sommerfeld effect along with the corresponding boost factor as functions of the DM mass. In section 4 we compare the model predictions for the hard positron and antiproton events with the experimental data. We conclude with a summary of our results in section 5.

## 2. SOMMERFELD ENHANCEMENT IN WINO DM MODEL

In MSSM with universal gaugino mass  $M_{1/2}$  at the GUT scale, the one-loop renormalized gaugino masses at weak scale are in the ratio,

$$M_1 : M_2 : M_3 :: \alpha_1 : \alpha_2 : \alpha_3 \simeq 1 : 2 : 7 \quad (1)$$

and the wino is not the LSP.

The wino LSP scenario is realized in the anomaly mediated supersymmetry breaking (AMSB) model [3–6], where the gaugino and scalar masses arise from supergravity breaking in the hidden sector via super-Weyl anomaly contributions. The gaugino masses are proportional to the gravitino mass  $m_{3/2}$

$$M_1 = \frac{33}{5} \frac{\alpha_1}{4\pi} m_{3/2}, \quad M_2 = \frac{\alpha_2}{4\pi} m_{3/2}, \quad M_3 = -3 \frac{\alpha_3}{4\pi} m_{3/2} \quad (2)$$

and the renormalised gaugino masses at the weak scale are in the ratio,

$$M_1 : M_2 : |M_3| :: \frac{33}{5} \alpha_1 : \alpha_2 : 3\alpha_3 \simeq 2.8 : 1 : 7.1 \quad (3)$$

In the minimal AMSB model the slepton masses come out negative at the weak scale , and this situation is ameliorated by adding a common scalar mass term  $m_0$  at tree level . This model has four free parameters,  $m_{3/2}, m_0, \tan\beta$  and  $\text{sgn}(\mu)$ . Besides the wino turns out to be the LSP in some string inspired models [7, 8]. Both the wino annihilation and the Sommerfeld enhancement processes of our interest are controlled by its isospin gauge coupling  $\alpha_2$  to  $W$  boson. So our results are essentially independent of the underlying SUSY model; and depend only on the wino LSP mass.

The scattering or annihilation cross section of non-relativistic particles in the initial state can be substantially changed if there is a long-range force between the incoming particles which distorts their wave function. The corrected cross section due to the distortion of incoming states from the plane wave can be calculated from the wave function of the two-body system in the attractive potential of the exchanged light particles. Taking  $M$  as the initial particles mass and  $m_\phi$  the exchanged boson mass and  $\alpha$  the coupling, the  $L=0$  partial wave obeys the Schrodinger equation

$$\frac{1}{M} \frac{d^2\psi}{dr^2} + \frac{\alpha}{r} e^{-m_\phi r} \psi = -Mv^2 \psi \quad (4)$$

with the boundary condition  $\psi'(r) = iMv\psi(r)$  and  $\psi(r) = e^{iMvr}$  at  $r \rightarrow \infty$ . The Sommerfeld enhancement factor is  $S = |\psi(\infty)|^2/|\psi(0)|^2$ . The Sommerfeld factor can be calculated by solving the Schrodinger equation (4) numerically [19–21] . In this paper we use an analytical approximation for the Sommerfeld factor which can be written as [23, 33, 34],

$$S(v, M, m_\phi) = \frac{\pi\alpha \sinh\left(\frac{12Mv}{\pi m_\phi}\right)}{v \left( \cosh\left(\frac{12Mv}{\pi m_\phi}\right) - \cos\left(2\pi\sqrt{\frac{6M\alpha}{\pi^2 m_\phi} - \frac{36M^2 v^2}{\pi^4 m_\phi^2}}\right) \right)} \quad (5)$$

The annihilation cross section of the S-wave initial states gets enhanced at low velocities by the factor  $S$ . For the  $W$  ladder processes taking  $m_\phi = M_W$  and  $\alpha = \alpha_2 = 1/30$ , the plots for  $S$  as a function of the DM mass  $M$  at different velocities is shown in Fig 1. We see that the maximum enhancement takes place at  $M \sim 4\text{TeV}$  for any given velocity.

The  $W$  ladder also gets corrections due to the  $\gamma$  and  $Z$  exchange between the chargino intermediate states. We follow [19] and ignore the corrections due to these extra channels which is a adequate approximation owing to the uncertainty in the knowledge about the velocity distribution of the DM. We shall see from the relic density calculation of the next section that the two narrow bands of wino masses  $M = (3.977 - 3.983) \text{ TeV}$  and  $M =$

(3.944 – 3.951) TeV are compatible with WMAP measurements at  $3\sigma$ . For the calculation of the boost factor relevant to PAMELA signal we take  $M = 3.98$  TeV (at the middle of the higher WMAP compatible band) and assuming the the galactic rms velocities  $v = 0.33 \times 10^{-3}$ , the Sommerfeld enhancement is  $S = 10^4$ . The velocity needed for the required boost factor is within the range observed in rotation curves of galaxies. It is possible that there are cold pockets in the galaxy where the rms velocities are lower ( $v \simeq 10^{-4}$ ), and in these cold pockets the DM annihilation can get a larger boost factor ( $S \simeq 10^5$ ) and they can make significant contribution to the PAMELA signals [19]. In that case the boost factor of  $10^4$  represents an average DM contribution from such cold clumps and the smooth halo, which is parameterized here via an effective velocity of  $0.33 \times 10^{-3}$ .

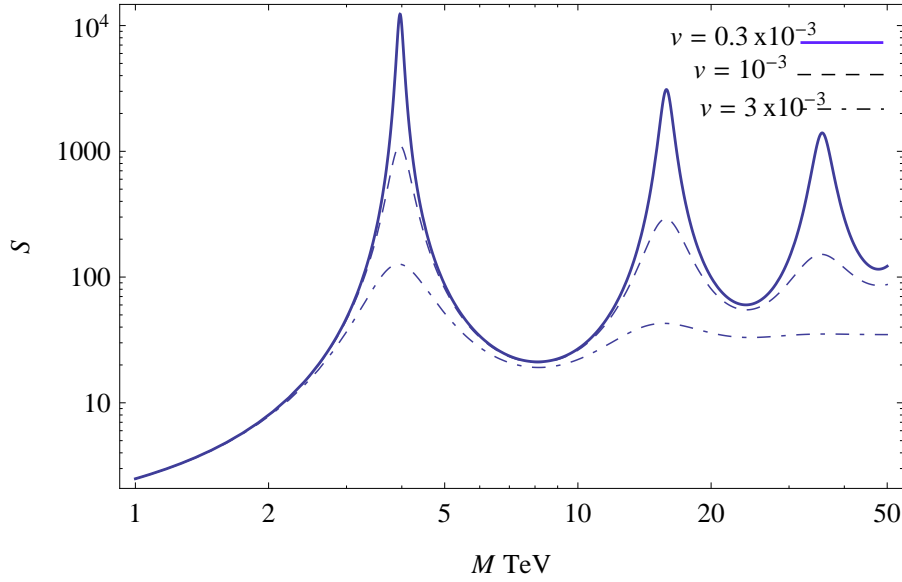


FIG. 1: Sommerfeld enhancement from  $W$  exchange as a function of the DM mass for different relative velocities.

For the calculation of relic density we use the relation (5) for  $S(v, M)$  to calculate the thermal average of the cross-section which is a function of the temperature  $T$  or  $x = M/T$ , by averaging the cross-section over all velocities at a given temperature,

$$\langle \sigma v \rangle = \frac{x^{3/2}}{2\sqrt{\pi}} \int_0^\infty dv (\sigma v) S(v, M) v^2 e^{-xv^2/4} \quad (6)$$

where  $v_{rel} = 2v$  is the relative velocity between the annihilating particles in the center of mass frame. This thermal averaged cross section is used in the calculation of relic abundance which we describe in the next section.

### 3. WINO RELIC DENSITY WITH SOMMERFELD FACTOR

The thermal averaged annihilation cross section  $\langle\sigma v\rangle(x)$  determines the relic density  $n_\chi$  through the Boltzman equation

$$\frac{dn_\chi}{dt} + 3Hn_\chi = -\langle\sigma v\rangle (n_\chi^2 - n_{\chi eq}^2) \quad (7)$$

where  $n_{\chi eq} = g_\chi(M^2/(2\pi x))^{3/2} e^{-x}$  is the the number density of  $\chi$  produced by the back-reaction  $ff' \rightarrow \chi\chi$  at a given temperature. The Boltzman equation can be written in terms of dimensionless variables  $Y_\chi = n_\chi/s$  (where  $s = (2\pi^2/45)g_{*s}T^3$  is the entropy density) and  $x$  as,

$$\frac{dY_\chi}{dx} = -\frac{\lambda(x)}{x^2} \left( Y_\chi^2(x) - Y_{\chi eq}^2(x) \right) \quad (8)$$

where

$$\lambda(x) \equiv \left( \frac{\pi}{45} \right)^{1/2} M M_{Pl} \left( \frac{g_{*s}}{\sqrt{g_*}} \right) \langle\sigma v\rangle(x) \quad (9)$$

where  $g_*$  and  $g_{*s}$  are the effective degrees of freedom of the energy density and entropy density respectively. The freeze-out temperature is defined as the solution of

$$Y(x_f) = (1+c)Y_{eq}(x_f) = (1+c)(0.145) \frac{g_\chi}{g_{*s}} x_f^{3/2} e^{-x_f} \quad ; \quad (10)$$

where the constant  $c \simeq 1$ ,  $g_\chi = 2$  for neutralinos; and the freeze-out temperature turns out to be given by  $x_f \simeq 20$ . Below the freeze-out temperature  $Y_{eq}(x)$  can be dropped from (8) and we can write the solution of (8) in the present epoch as

$$\frac{1}{Y(x_s)} = \frac{1}{Y(x_f)} + \int_{x_f}^{x_s} dx \frac{\lambda(x)}{x^2} \quad (11)$$

where  $x_s$  is the temperature where the co-moving density of  $\chi$  does not change noticeably and the integration can be terminated. The DM density fraction in the present universe is then given by

$$\Omega = \frac{Y(x_s) s_0 M}{\rho_c} \quad (12)$$

where  $s_0 = 2918\text{cm}^{-3}$  is the entropy of the present universe and  $\rho_c = h^2 8.1 \times 10^{-47} \text{GeV}^4$  is the critical density. The observed value of CDM density from the seven year WMAP data is  $\Omega_c h^2 = 0.1123 \pm 0.0105$  ( $3\sigma$ ) [24] (where  $h$  is the Hubble parameter in units of 100 km/s/Mpc).

From the calculation of relic density in the wino LSP models [9] it is known that the WMAP relic density  $\Omega_c h^2 = 0.1123 \pm 0.007(2\sigma)$  is attained if the wino mass is in the range

$M_2 = (2.1 - 2.3)\text{TeV}$ . A wino mass of 4 TeV results in an overabundance by a factor of 3 larger than the WMAP limit.

In the following we calculate the relic density of WINO LSP by including the Sommerfeld factor in the annihilation cross section. In [35] an approximate form of Sommerfeld factor was included in the annihilation cross section and it was found that wino mass which gave the correct relic density was in the range  $M_2 = (2.7 - 3.0)\text{TeV}$ .

In this paper we incorporate the Sommerfeld effect following Feng et al [22, 23], taking into account the fact that the DM particles do not share the same temperature with radiation bath below a the kinetic decoupling temperature but in fact cool faster than radiation. The Sommerfeld factor becomes very effective at temperatures below kinetic decoupling, and that solves the problem of DM overabundance at  $M=4$  TeV.

For the wino DM, the annihilation channels are  $\chi^0\chi^0 \xrightarrow{\chi^+} W^+W^-$  with a cross section [35]

$$(\sigma v) = \frac{2\pi \alpha_2^2}{M^2} \quad (13)$$

and the dominant co-annihilation channel  $\chi^0\chi^- \xrightarrow{W^-} ff'$  with the cross section for the S-wave initial state

$$(\sigma v) = \frac{1}{2} \frac{\pi \alpha_2^2}{M^2} \quad (14)$$

The chargino-neutralino mass difference is  $\Delta M \simeq 200\text{MeV}$  [5, 41], so the co-annihilation channel will not take place below  $\Delta M \simeq (3/2)T$  or  $T = 133.3\text{MeV}$ .

**Kinetic decoupling:** It has long been recognized that after the freezeout the dark matter distribution at some point will not have the same temperature as the radiation bath but cool more rapidly[36–38]. It has also been pointed out that in cases where the DM annihilation has strong velocity dependent cross sections as in the case of Sommerfeld effect the kinetic decoupling of DM will result in rapid annihilation of DM much below the freeze-out temperature [22, 23, 39, 40]. In this section we calculate the temperature of kinetic decoupling of heavy wino DM and incorporate it in the wino relic density calculation.

The  $\chi_0$  DM will have the same temperature as the radiation bath of standard model particles till the rate of momentum transfer due to scattering

$$\Gamma_k = n_r \langle \sigma v \rangle \frac{T}{M} \quad (15)$$

is larger than the Hubble expansion rate  $H = 1.66\sqrt{g_*}T^2/M_{Pl}$ . The kinetic decoupling temperature  $T_{kd}$  is defined as the temperature where  $\Gamma_k(T_{kd}) = H(T_{kd})$ . For  $T > M_W$

the scattering process  $\chi_0 W^+ \xrightarrow{\chi^+} \chi_0 W^+$  has a cross section  $\langle \sigma v \rangle = 2\alpha_2^2/M^2$  and the kinetic decoupling condition gives the kinetic decoupling temperature to be

$$T_{kd}^W = 2.5 \times \left( \frac{M^3}{\alpha_2^2 M_{Pl}} \right)^{1/2} = 5.4 \text{MeV} \left( \frac{M}{4 \text{TeV}} \right)^{3/2}. \quad (16)$$

But at this temperature there are no  $W^\pm$  in the radiation bath, so the kinetic decoupling temperature for this interaction channel is  $T_{kd}^W = (2/3)M_W = 54 \text{GeV}$ .

Other processes that maintain temperature equality between the DM and the radiation bath are the elastic scattering with relativistic fermions,  $f\chi^0 \rightarrow f\chi^0$ . In the absence of a Higgsino component in the DM there is no  $Z$  exchange diagram, and the elastic scattering process will come from s and u-channel sfermion exchanges with the cross section [37],

$$\langle \sigma v \rangle = 12\pi\alpha_2^2 I_f^4 \frac{E_f^2}{(M_{\tilde{f}}^2 - M^2)^2} \quad (17)$$

where  $I_f$  is the isospin of  $f$ ,  $M_{\tilde{f}}$  is the sfermion mass and  $E_f = (3/2)T$  is the fermion energy. The kinetic decoupling temperature of the relativistic fermion-wino scattering process will then be given by

$$T_{kd}^f = 4.2 \left( \frac{(M_{\tilde{f}}^2 - M^2)^2 M}{M_{Pl}} \right)^{1/4} \quad (18)$$

If we take  $M = 4 \text{TeV}$  and  $M_{\tilde{f}} = 10 \text{TeV}$ , then the kinetic decoupling for this channel takes place at  $T_{kd}^f = 5.2 \text{GeV}$  while for  $M_{\tilde{f}} = 5 \text{TeV}$ ,  $T_{kd}^f = 1.7 \text{GeV}$ .

Finally the quasi-elastic scattering  $\chi^0 f \xleftrightarrow{W} \chi^\pm f'$  will maintain the kinetic-coupling of  $\chi^0$  with radiation down to a temperature  $T = (2/3)\Delta M = 133 \text{MeV}$ , assuming a typical charged and neutral wino mass difference  $\Delta M = 200 \text{ MeV}$  [5, 41]. Below the temperature  $133 \text{MeV}$  there will be no charginos in the heat bath so the kinetic decoupling of the winos from the heat bath will take place at  $T_{kd} = 133 \text{MeV}$ . Since this is the lowest of the kinetic decoupling temperatures from various processes discussed above, we will take  $T_{kd} = 133 \text{MeV}$  for the calculation of wino relic abundance. In Fig 2 we show the effect of the kinetic decoupling temperature on the relic density. Early de-couplings enhance the annihilation and lower the relic abundance. We take  $T_{kd} = 133 \text{MeV}$  as the effective kinetic decoupling temperature for calculating the relic abundance.

At temperatures below  $T_{kd}$  the temperature of the decoupled non-relativistic particles is related to their momenta as  $(3/2)T = Mv^2/2$ . As the velocities of NR particles in the expanding universe goes down with the scale factor as  $v \propto 1/a$ , DM temperature falls with

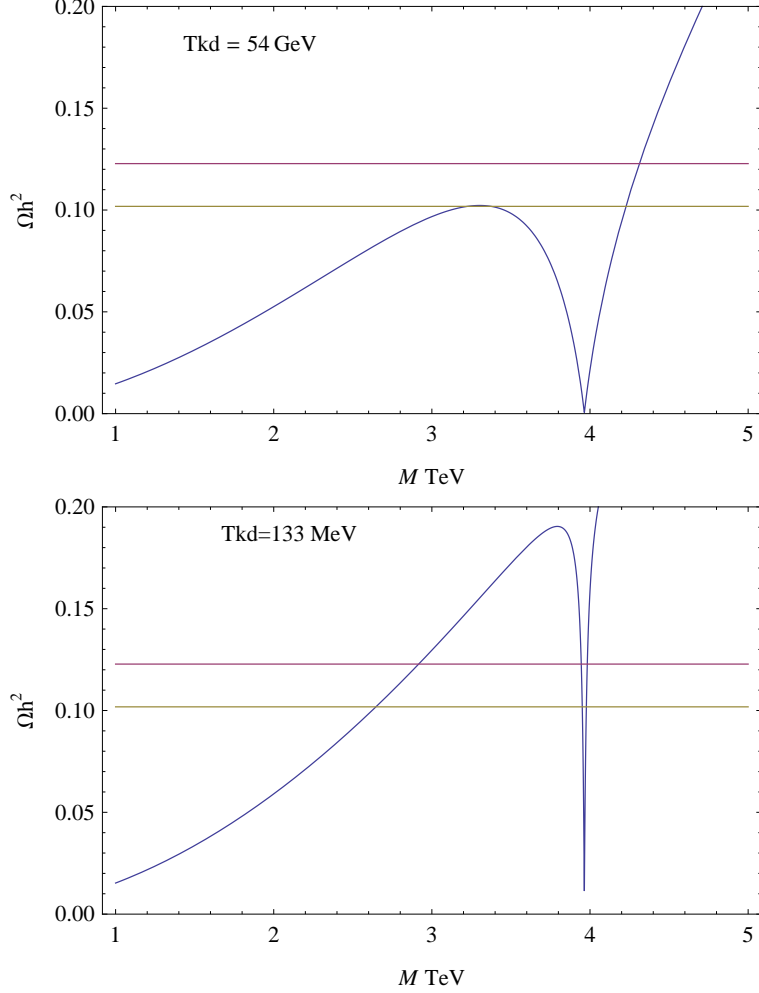


FIG. 2: Wino relic density with Sommerfeld enhancement with two different kinetic decoupling temperatures as discussed in the text.  $T_{kd} = 133\text{MeV}$  (bottom panel) is assumed for the wino relic density calculation. The  $3\sigma$  band of WMAP relic density [24] is indicated by the horizontal lines.

the scale factor as  $1/a^2$  while the radiation temperature goes as  $1/a$ . The integration in (eqn. 11) in the interval  $x > x_{kd} \equiv M/T_{kd}$  is performed by replacing  $x$  in the integrand by  $x^2/x_{kd}$ , which corresponds to the temperature of the DM particles. This is because the thermal equilibrium in this region is maintained by scattering between DM particles via multiple W boson exchange (Sommerfeld ladder) i.e  $\chi^0\chi^0 \xleftrightarrow{W} \chi^+\chi^-$ . Thanks to the Sommerfeld effect this process can continue for  $T < T_{kd}(133\text{ MeV})$ . The rapid reduction in velocities or temperatures of DM particles below the kinetic decoupling temperatures results in a large enhancement in the annihilation cross section and reduction of the relic abundance in the late universe ( $T < T_{kd}$ ). With these inputs we carry out the integration in equation (11)

numerically to obtain  $Y(x_s)$ . We plot  $Y(x_s)$  in Fig 3 and find that  $Y(x_s)$  remains constant after  $x_s > 4 \times 10^7$  which corresponds to the temperature  $\sim 100 \text{keV}$ . Below this temperature there is a chemical decoupling of the winos in the sense that their comoving abundance remains constant. This can be physically understood as follows. In the range  $x_{kd} < x < x_s$ , the DM particles are kept in thermal equilibrium by their mutual scattering  $\chi^0 \chi^0 \xleftrightarrow{W} \chi^+ \chi^-$ . But at  $x > x_s$  the scattering rate for this process falls below the Hubble expansion; so the DM particles no longer maintain a Maxwell-Boltzmann thermal distribution. Consequently the low velocity particles with enhanced annihilation rate (5) are decoupled from the high velocity particles. The latter escape annihilation, leading to a constant comoving abundance of DM at  $x > x_s$  and this process is called chemical decoupling.

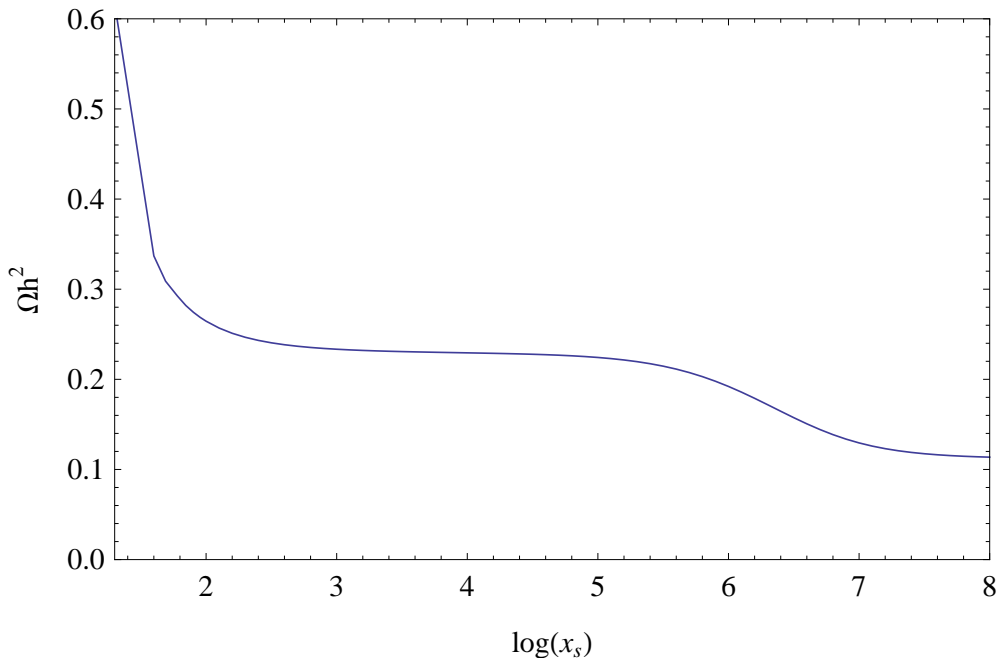


FIG. 3: Relic density as a function of cutoff temperature  $x_s$  for a wino DM mass  $M=4 \text{ TeV}$ . There is a fall at  $x_s = 10^5$  due to kinetic decoupling, and the chemical decoupling occurs at  $x_s = 4 \times 10^7$ .

In Fig 4 we show the relic density as a function of wino mass close to the Sommerfeld resonance. We see that two narrow bands of wino masses  $M = (3.977 - 3.983) \text{TeV}$  and  $M = (3.944 - 3.951) \text{TeV}$  are compatible with WMAP measurements at  $3\sigma$ . Admittedly there is fine-tuning involved in reproducing the WMAP relic density with the Sommerfeld resonance. In the absence of a unique measure of fine-tuning, however, we have not given a numerical estimate of this quantity. Instead we have presented this fine-grained plot from

which the interested reader can estimate the fine-tuning measure of his choice.

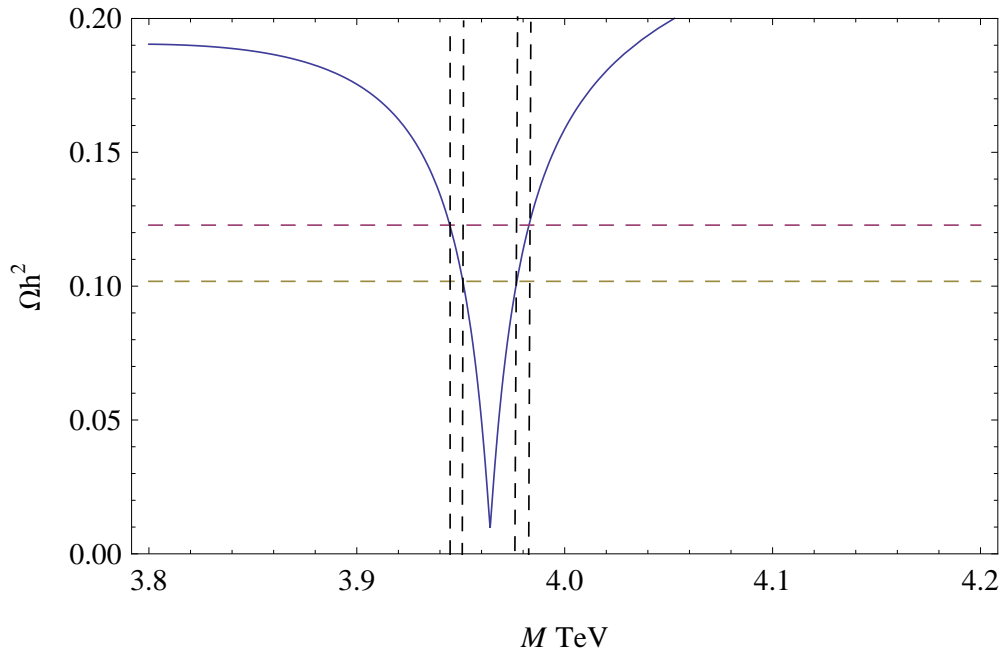


FIG. 4: Plot shows the relic density as a function of wino mass close to the Sommerfeld resonance. We see that two narrow bands of wino masses  $M = (3.977-3.983)\text{TeV}$  and  $M = (3.944-3.951)\text{TeV}$  are compatible with WMAP measurements at  $3\sigma$ .

Fig. 5 shows Sommerfeld enhancement  $S$  for the range of  $M = (3.977-3.983)\text{ TeV}$  as a function of velocity. A Sommerfeld enhancement factor of  $S = 10^4$  is obtained for  $v = 0.33 \times 10^{-3}$  and  $M=3.98\text{TeV}$ .

We choose the central values  $M = 3.98\text{TeV}$  (which is the center of the higher mass band) to compute the positron, electron, antiproton and diffuse  $\gamma$ -ray flux to compare with the observations of PAMELA and Fermi-LAT .

#### 4. COMPARISON WITH PAMELA AND FERMI-LAT DATA

The satellite based PAMELA experiment measures the flux spectrum of  $e^+/(e^+ + e^-)$  [1] in the energy range of  $(10 - 100)\text{ GeV}$  and  $\bar{p}/p$  [25, 26] in the range  $(1 - 180)\text{GeV}$ . It is found that the  $e^+/(e^+ + e^-)$  ratio exceeds the flux estimated from astrophysical sources by a large margin at higher energies. However the  $\bar{p}$  flux is within the expected range of what is expected of secondary  $\bar{p}$  produced from the primary CR protons from AGN's and other

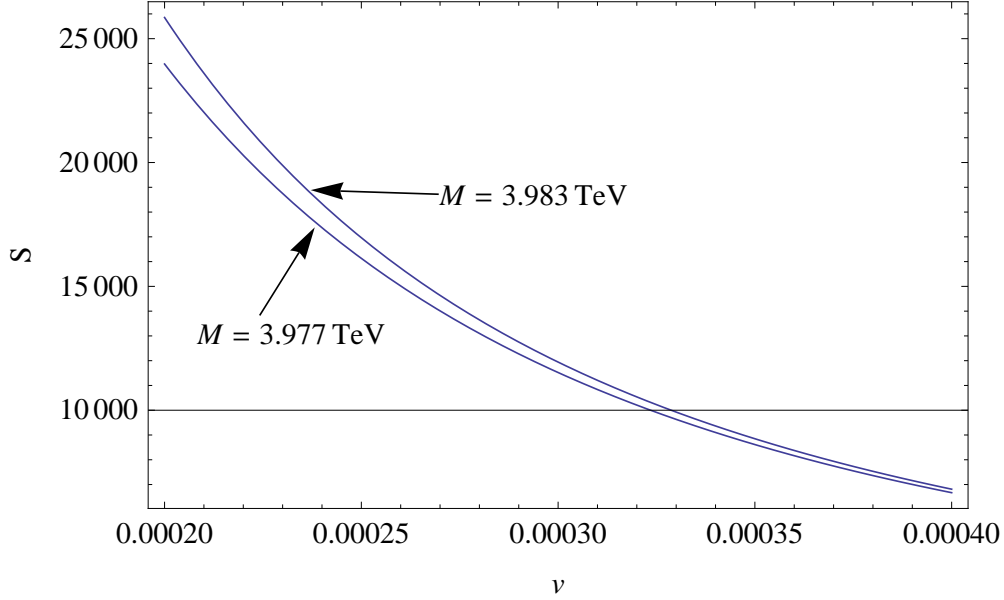


FIG. 5: Sommerfeld enhancement  $S$  for the range of  $M = (3.977-3.983)$  TeV (compatible with WMAP relic density) as a function of velocity. A Sommerfeld enhancement factor of  $S = 10^4$  is obtained for  $v = 0.33 \times 10^{-3}$  and  $M=3.98\text{TeV}$ .

sources. Any DM annihilation or decay model must explain the large flux of positrons and the paucity of  $\bar{p}$ 's in the PAMELA signal. In addition there are measurements of  $(e^+ + e^-)$  and  $\gamma$ -rays in the by Fermi-LAT [27, 28, 32], and the DM signal must be consistent with the Fermi-LAT data [42–48]. In this section we check the predictions of the heavy wino DM model with the PAMELA and Fermi-LAT data.

We use the MicrOMEGAs [49] to calculate rate of of positrons and antiprotons produced by the annihilation of 3.98 TeV wino DM. As input we take the following SUSY parameters  $\mu = 9$  TeV,  $M_2 = 3.837$  TeV and the other gauginos in the ratio  $M_1 : M_2 : M_3 = 2.8 : 1 : 7.1$  while the squark and slepton masses  $M_{\tilde{q}} = M_{\tilde{f}} = 10$  TeV. We take  $\tan\beta = 10$  and  $\mu = 9\text{TeV}$ . As mentioned earlier, however, the results are insensitive to all the SUSY parameters other than the LSP mass. We calculate the annihilation cross section of a 3.98 TeV wino LSP and the branching spectrum ( $\frac{dN}{dE}$ ) into electrons, positrons, antiprotons and photons using MicroOMEGAs. We fit the positron and antiproton spectrum from MicrOMEGAs with an analytical functions which is then input in the GALPROP code to calculate the observed fluxes.

$L$ (kpc)	$D_{0xx}$ ( $10^{28} \text{ cm}^2$ )	$\delta$	$V_a$ (km/s)	$\frac{\partial V_c}{\partial z}$ (km/s/kpc)	$\gamma_n$	$\gamma_e$	$N_p$ at 100 GeV $\text{MeV}^{-1}\text{cm}^{-2}\text{s}^{-1}\text{sr}^{-1}$	$N_e$ at 34.5 GeV $\text{MeV}^{-1}\text{cm}^{-2}\text{s}^{-1}\text{sr}^{-1}$	S
2.0	2.83	0.34	33.67	0.5	2.36	2.5	$3.5 \times 10^{-9}$	$0.4 \times 10^{-9}$	10000

TABLE I: Diffusion parameters and boost factor used as input in GALPROP.

For electrons/positrons we use

$$\left(\frac{dN_e}{dE_e}\right) = E_e^{-1} \left[ 5 \exp \left[ - \left( 0.018 \frac{E_e}{M_\chi} \right)^{1.5} \right] - \left( \frac{E_e}{M_\chi} \right)^{-0.4} + 0.3 \right], \quad (19)$$

while for protons/antiprotons the we use the analytical fit,

$$\left(\frac{dN_p}{dE_p}\right) = E_p^{-1} \left[ 5.5 \left( \frac{E_p}{M_\chi} \right)^4 \exp \left[ -6.35 \left( \frac{E_p}{M_\chi} \right)^{0.25} \right] - 3 \times 10^{-6} \left( \frac{E_p}{M_\chi} \right) \right] \quad (20)$$

and for  $\gamma$ -ray spectrum we use

$$\left(\frac{dN_\gamma}{dE_\gamma}\right) = E_\gamma^{-1} \left[ 2000 \left( \frac{E_\gamma}{M_\chi} \right)^{1.8} \exp \left[ -5 \left( \frac{E_\gamma}{M_\chi} \right)^{0.24} \right] \right] \quad (21)$$

where  $E_e$ ,  $E_p$  and  $E_\gamma$  are in units of MeV, while  $M_\chi \simeq 4 \text{ TeV}$ . The integrated number of electrons/positrons, antiprotons and photons per wino pair annihilation are  $N_e = 14.2$ ,  $N_p = 1.59$  and  $N_\gamma = 26$  respectively. We show the result of the output from MicrOMEGAs along with our analytical fits (19,20) and 21 in Fig 6.

The cross section from MicrOMEGAs of the wino annihilation to  $W^+W^-$  is  $5.63 \times 10^{-27} \text{ cm}^3/\text{s}$ . We use the Galactic propagation code GALPROP [50, 51] to obtain the positron and antiproton fluxes at the earth. We input a boosted cross section  $(\sigma v)_0 S = 5.63 \times 10^{-23} \text{ cm}^3/\text{s}$  in the GALPROP code along with the analytical fits of  $(dN/dE)$  (19,20). We choose the isothermal dark matter distribution profile [52] and calculate the flux of  $e^+$ ,  $e^-$ ,  $p$ ,  $\bar{p}$  on earth arising from the wino annihilation in the galaxy.

These inputs from MicroOmegas goes into the the source term

$$q(\vec{r}, p) = \langle \sigma v \rangle_0 S \frac{\rho}{M^2} \left( \frac{dN}{dE} \right) \quad (22)$$

of the propagation equation for the cosmic ray density (at galactic radius  $r$  and with momentum  $p$ ) [51],

$$\frac{\partial \psi(\vec{r}, p)}{\partial t} = q + \vec{\nabla} \cdot (D_{xx} \vec{\nabla} \psi - \vec{V}_c \psi) + \frac{\partial}{\partial p} p^2 D_{pp} \frac{\partial}{\partial p} \frac{1}{p^2} \psi - \frac{\partial}{\partial p} \left[ \dot{p} \psi - \frac{p}{3} (\vec{\nabla} \cdot \vec{V}_c) \psi \right] - \frac{1}{\tau_f} \psi - \frac{1}{\tau_r} \psi \quad (23)$$

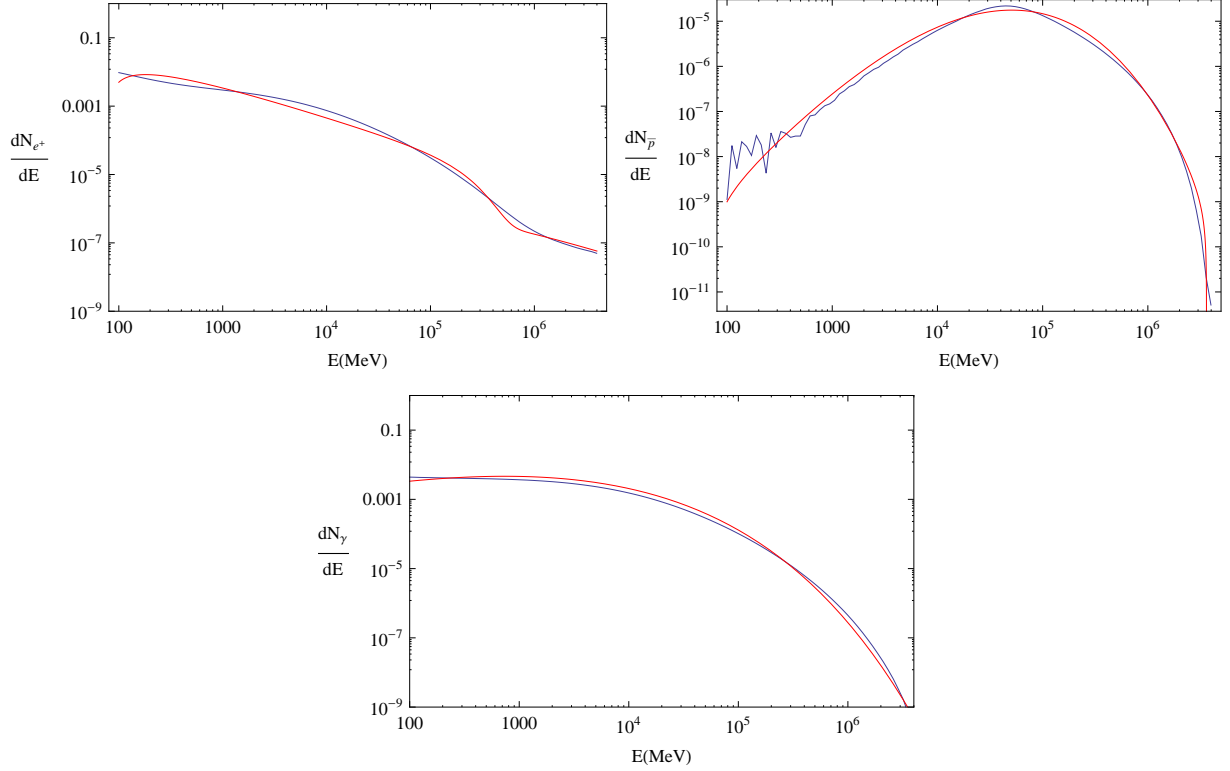


FIG. 6: Top left panel shows positron spectrum, top right panel shows antiproton spectrum and bottom panel shows gamma ray spectrum from wino annihilation. Light shaded curve shows the fitted functions (19, 20) and 21.

where  $D_{xx}$  is the diffusion coefficient which describes the scattering of CR by the random galactic magnetic fields,  $V_c$  is the convection velocity of the bulk CR in the galaxy (and this term represents the scattering of the CR by the background CR "wind"),  $D_{pp}$  is the diffusion coefficient in momentum space (which represents acceleration in turbulent B fields),  $\dot{p}$  is the energy loss due to radiative decay and the final two terms represent the possible fragmentation or radioactive decay of the CR nuclei. This equation is solved over a diffusion zone represented by a cylinder whose origin and axis coincide with our galactic disk. The half height of this cylinder is typically  $L \sim 1 - 10$  kpc [46]. The energy dependent diffusion coefficient is parameterized as  $D_{xx}(\vec{r}, E) = D_{0xx}E^\delta$ . The primary spectrum for all nuclei is parameterized as[46]

$$\psi = \frac{N}{2} \frac{L}{D_{0xx}} E^{-\gamma_n - \delta} \quad (24)$$

and a similar expression for electrons with  $\gamma_n$  replaced by  $\gamma_e$ . For a given set of input parameters characterizing the primary spectra for any CR species, the GALPROP code

propagates the CR flux and gives the flux observed at the earth. We choose the set of parameters  $D_{0xx}, L, V_c, \delta, V_a$  (Alfven velocity),  $\frac{\partial V_c}{\partial z}, \gamma_n$  (tabulated in Table.I) which gives the Boron/Carbon ration in CR consistent with measurements by HEAO-3 [29], ATIC-2 [30] and CREAM [31] experiments as shown in Fig7. This is not the only parameter set which gives the correct B/C spectrum, but in our scan of parameters we find that this set gives a smallest contribution to the  $\bar{p}/p$  flux ratio.

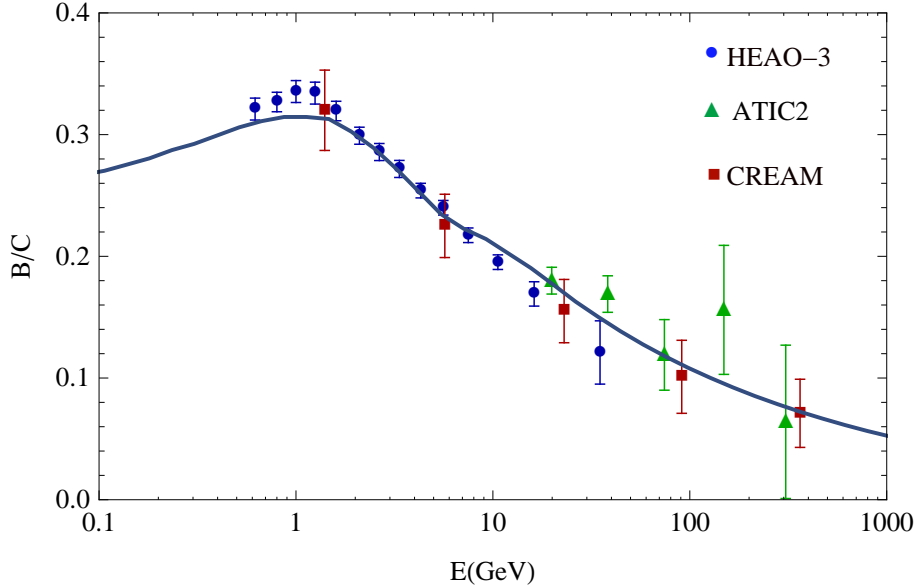


FIG. 7: Boron/Carbon ratio for the assumed galactic diffusion parameters shown in Table 1. compared with data from HEAO-3 [29], ATIC-2 [30] and CREAM [31] experiments.

The primary-electrons spectral index  $\delta_e = 2.5$  is chosen to fit the Fermi ( $e^+ + e^-$ ) data. The primary proton flux  $N_p$  and electron flux  $N_e$  are also fixed by fitting with the ( $e^+ + e^-$ ) and  $B/C$  observations. This set of parameters fixes the background  $\bar{p}/p$ ,  $e^- + e^+$  and the  $\gamma$ -ray photon. In Fig.8 we show the ( $e^+ + e^-$ ) signal from the 3.98 TeV wino DM model with observations from Fermi-LAT [27, 28].

With the parameters for the background thus fixed we vary the boost factor trying to get a fit for the ( $e^+/(e^+ + e^-)$ ) data while at the same time being consistent with the  $\bar{p}/p$  data. We find that the boost factor  $S = 10^4$  gives a good fit to the PAMELA positron data with a  $\chi^2/d.o.f = 1.03$  while being consistent with the PAMELA antiproton data (with  $\chi^2/d.o.f = 1.68$ ). The large DM mass helps to ameliorate the discrepancy with the PAMELA antiproton data by pushing up the predicted peak to still higher energies.

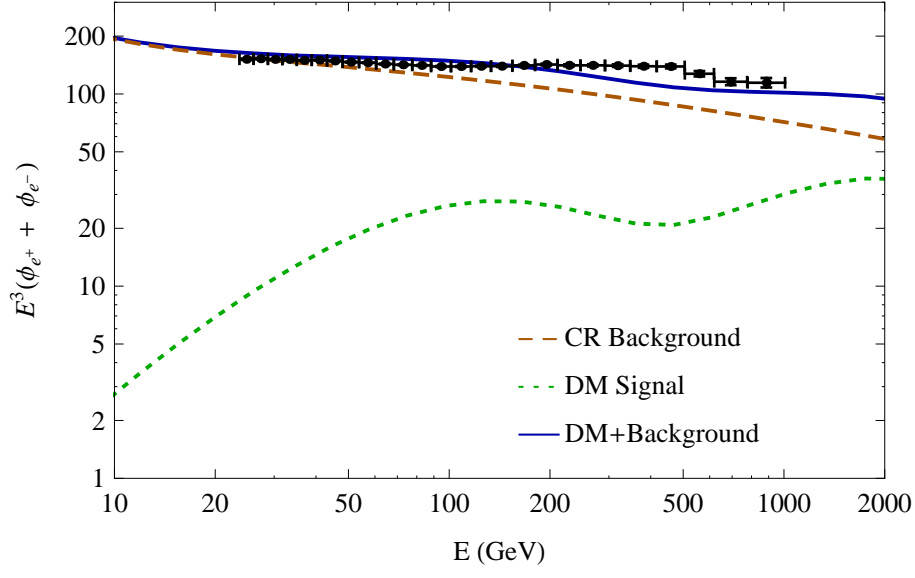


FIG. 8: The  $(e^- + e^+)$  flux for the 3.98 TeV wino DM compared with FERMI-LAT data [27, 28]. Dashed denotes the CR background and dotted line is the DM annihilation signal.

The total flux of positrons and antiprotons from the background as above plus the DM signal taken from GALPROP is shown in Fig 9 and Fig 10 respectively.

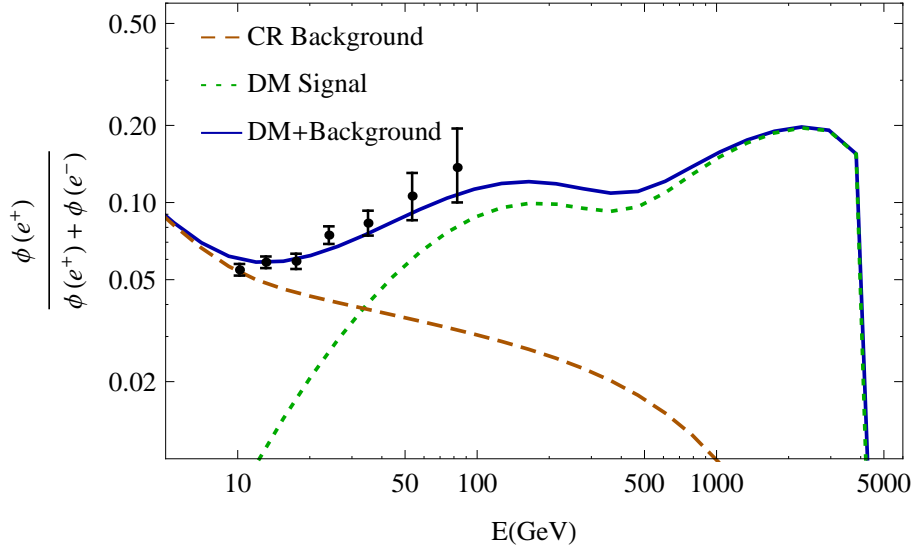


FIG. 9: Positron flux ratio for the 3.98 TeV wino DM compared with Pamela data [1]. Dashed line shows background from cosmic ray secondary positrons.

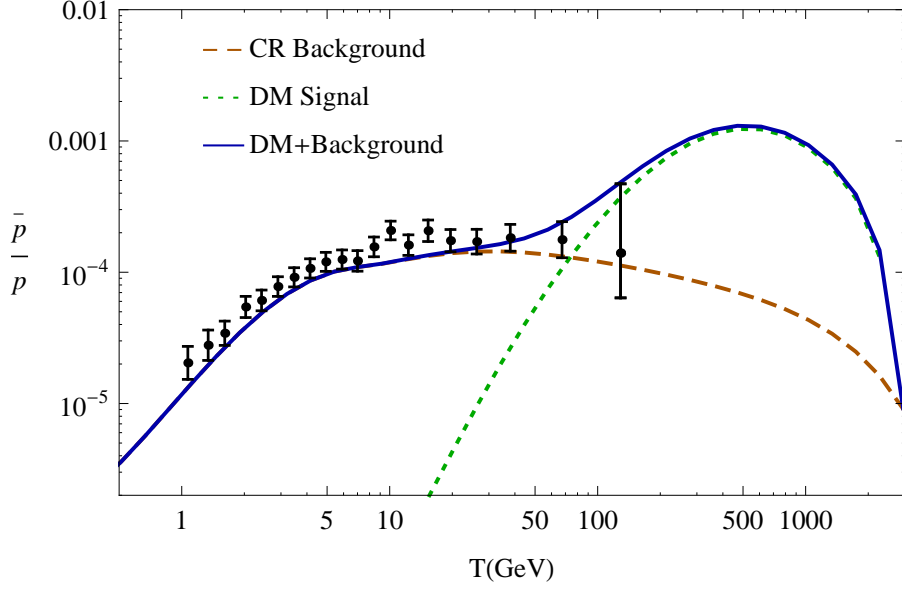


FIG. 10: Antiproton/Proton flux ratio for the 3.98 TeV wino DM compared with Pamela data [25, 26]. Dashed line shows background from cosmic ray secondary antiprotons while dotted line shows DM signal.

The  $\gamma$ -ray spectrum observed at earth from DM annihilation photons is given by

$$\Phi_\gamma = \frac{1}{4\pi} \langle \sigma v \rangle_0 S \frac{dN_\gamma}{dE_\gamma} \int_\Delta \Omega d\Omega \int_{los} \rho^2(l) dl \quad (25)$$

where  $\rho(l)$  is the DM density along the line of sight (los). In addition to the prompt photons from DM, photons are generated also by synchrotron radiation, inverse-Compton scattering from the CMB and infrared starlight from the primary electrons. The prompt photons are sensitive to the large scale DM distribution function  $\rho(l)$  along the line of sight. We find that the Isothermal distribution [52] gives a smaller gamma-ray flux compared to other DM profiles like NFW [53], Moore [55] or Einasto [54]. We plot the diffuse  $\gamma$ -ray flux for the  $M = 3.98\text{TeV}$  wino model for both the NFW ,

$$\rho_{NFW} = \rho_0 \frac{r_s}{r} \left( 1 + \frac{r}{r_s} \right)^{-2}, \quad \rho_0 = 0.26\text{GeV}/\text{cm}^3, r_s = 20\text{kpc}, \quad (26)$$

as well as the isothermal profiles

$$\rho_{ISO} = \rho_\odot \frac{1 + (\frac{r_\odot}{r_s})^2}{1 + (\frac{r}{r_s})^2}, \quad \rho_\odot = 0.3\text{GeV}/\text{cm}^3, r_\odot = 8.5\text{kpc}, r_s = 5\text{kpc}, \quad (27)$$

The local DM density for both profiles is  $\rho_\odot = 0.3\text{GeV}/\text{cm}^3$  and  $r_s$  is the size of the DM halo. In Fig.11 we show the plots for the integrated  $\gamma$ -ray signal at large galactic latitudes

$b > 20^\circ$  observed by Fermi-LAT [32]. The  $\gamma$ -ray signal from 3.98 TeV wino annihilation is consistent with measurements from Fermi-LAT. At lower energies the primary contribution to the  $\gamma$ -ray flux is from astrophysical sources like gamma ray blazars and intergalactic shock waves from structure formation [56], which is beyond the scope of the present work.

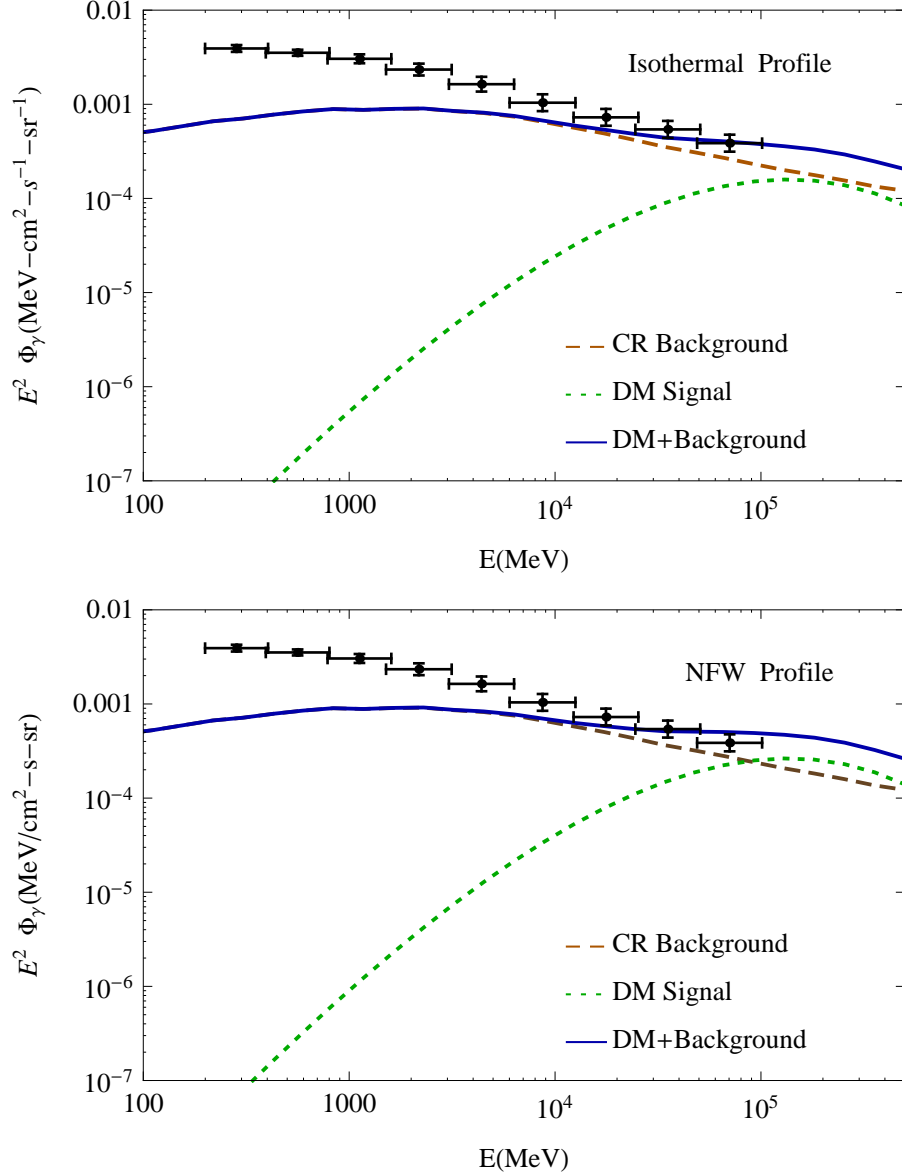


FIG. 11: Diffuse  $\gamma$ -ray flux for the 3.98 TeV wino DM compared with FERMI-LAT integrated  $\gamma$ -ray flux at galactic latitudes  $b > 20^\circ$  [32]. Dashed line shows background. The prompt photon signal is smaller in the isothermal profile (top panel) compared to the NFW profile (bottom panel). At lower energies the primary contribution to the  $\gamma$ -ray flux is from astrophysical sources like GRB's, gamma ray pulsars and AGN's which is beyond the scope of the present work.

Recent results from HESS reported diffuse  $\gamma$ -ray flux measurements from the galactic centre [57]. We show the effect of the Isothermal and NFW profiles on the results from HESS in Fig. 12. For both these profiles the DM signal is in the acceptable range although for NFW it is much larger than that for the Isothermal profile. This is due to the fact that the NFW profile is more sharply peaked at the galactic centre compared to the isothermal profile.

In this paper we have taken into account the non-perturbative effect of the W exchange in the initial state which results in the Sommerfeld enhancement in the cross section. It has been seen that the electroweak corrections in the final states and the bremsstrahlung of W and Z from the external legs in TeV scale DM annihilation can increase the cross section by a factor  $(1 + \alpha_2 \ln^2(M^2/M_W^2))$  [58, 59]. This increase in the effective cross section by  $\sim 30\%$  can be broadly taken into account in our analysis by reducing the necessary Sommerfeld enhancement by a corresponding factor of 1.3. There are interesting signals of Sommerfeld enhancement of the DM annihilation cross section in the CMB anisotropy [60, 61], and they can be pursued as potential signals of heavy wino DM which may be observed in the PLANCK [62] CMB anisotropy measurements.

## 5. CONCLUSIONS

We have investigated the possibility of reconciling the predictions of a heavy wino dark matter model with the WMAP data on relic density as well as the hard positron signal reported by the PAMELA experiment via the Sommerfeld enhancement factor. We find that they can be simultaneously explained if one assumes the wino mass to be very close to the Sommerfeld resonance mass of about 4 TeV. In that case the large Sommerfeld enhancement of dark matter annihilation cross-section below the freeze-out temperature reduces the present dark matter relic density to the range of the WMAP measurement. Moreover the Sommerfeld enhancement can boost the present dark matter annihilation cross-section by a large factor of about  $10^4$ , as required to explain the size of the PAMELA positron signal. At the same time the large DM mass helps to ameliorate the discrepancy with the PAMELA antiproton data by pushing up the predicted peak to still higher energies. We also find that the model predictions for  $(e^+ + e^-)$  and gamma-ray signals are broadly compatible with the Femi-LAT observations.

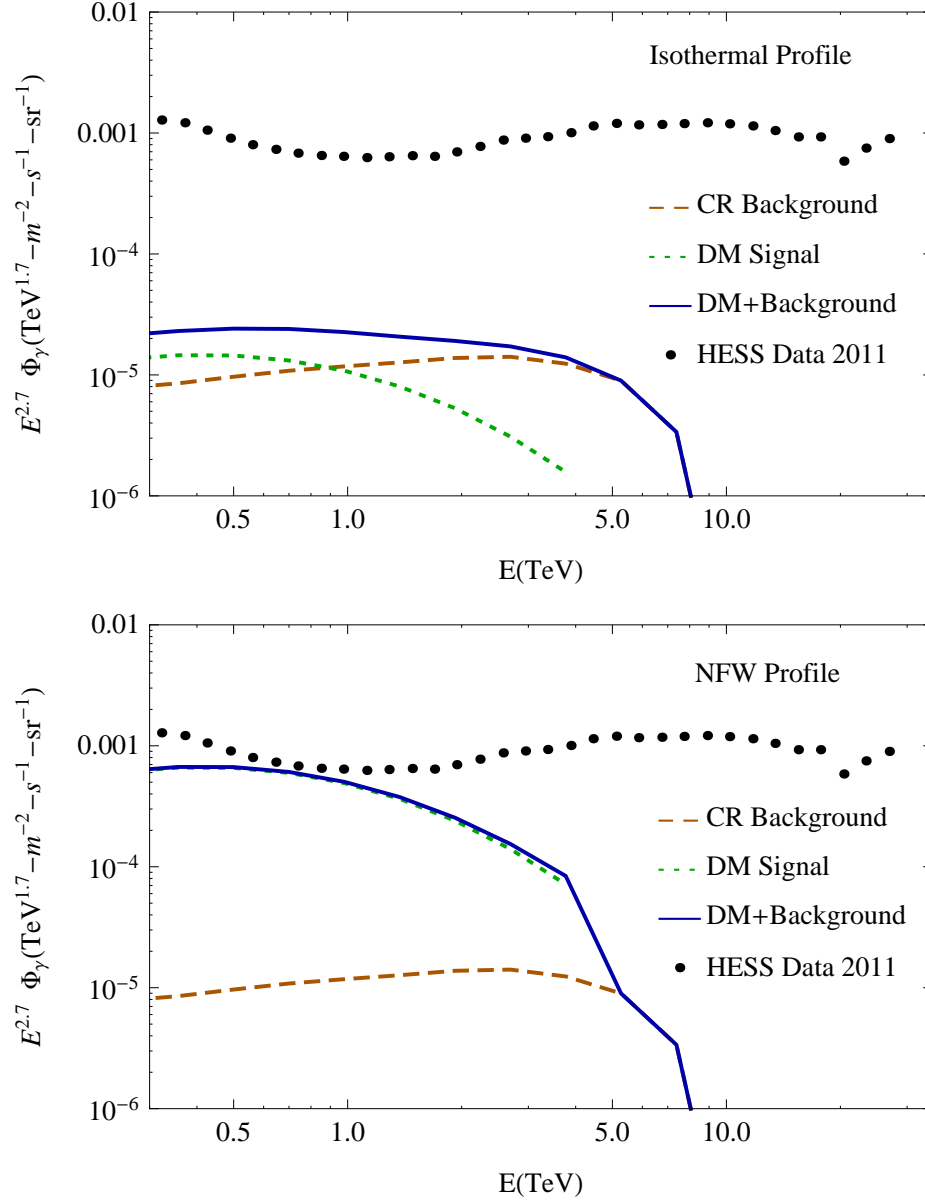


FIG. 12: Diffuse  $\gamma$ -ray flux for the 3.98 TeV wino DM compared with HESS [57] integrated  $\gamma$ -ray flux from a circular region of  $1^\circ$  centred around the galactic centre(GC). The DM signal from the GC is much smaller in the isothermal profile(top panel) compared to the NFW profile(bottom panel).

## 6. ACKNOWLEDGEMENTS

We thank Manuel Drees for many helpful comments and discussions. DPR acknowledges partial financial support from INSA under the senior scientist scheme. This work was started

as a working group project during WHEPP XI at PRL, Ahmedabad and advanced further during the NIUS Summer camp at HBCSE(TIFR), Mumbai.

- 
- [1] O. Adriani *et al.* [PAMELA Collaboration], Nature **458**, 607 (2009) [arXiv:0810.4995 [astro-ph]].
  - [2] M. Cirelli, M. Kadastik, M. Raidal and A. Strumia, Nucl. Phys. B **813**, 1 (2009) [arXiv:0809.2409 [hep-ph]].
  - [3] L. Randall and R. Sundrum, Nucl. Phys. B **557**, 79 (1999) [arXiv:hep-th/9810155].
  - [4] G. F. Giudice, M. A. Luty, H. Murayama and R. Rattazzi, JHEP **9812**, 027 (1998) [arXiv:hep-ph/9810442].
  - [5] T. Gherghetta, G. F. Giudice and J. D. Wells, Nucl. Phys. B **559**, 27 (1999) [arXiv:hep-ph/9904378].
  - [6] J. D. Wells, Phys. Rev. D **71**, 015013 (2005) [arXiv:hep-ph/0411041].
  - [7] A. Brignole, L. E. Ibanez and C. Munoz, Nucl. Phys. B **422**, 125 (1994) [Erratum-ibid. B **436**, 747 (1995)] [arXiv:hep-ph/9308271].
  - [8] J. A. Casas, A. Lleyda and C. Munoz, Phys. Lett. B **380**, 59 (1996) [arXiv:hep-ph/9601357].
  - [9] U. Chattopadhyay, D. Das, P. Konar and D. P. Roy, Phys. Rev. D **75**, 073014 (2007) [arXiv:hep-ph/0610077].
  - [10] V. Barger, W. Y. Keung, D. Marfatia and G. Shaughnessy, Phys. Lett. B **672**, 141 (2009) [arXiv:0809.0162 [hep-ph]].
  - [11] F. Donato, D. Maurin, P. Brun, T. Delahaye and P. Salati, Phys. Rev. Lett. **102**, 071301 (2009) [arXiv:0810.5292 [astro-ph]].
  - [12] I. Cholis, arXiv:1007.1160 [astro-ph.HE].
  - [13] J. Hisano, S. Matsumoto, O. Saito and M. Senami, Phys. Rev. D **73**, 055004 (2006) [arXiv:hep-ph/0511118].
  - [14] J. Hisano, S. Matsumoto and M. M. Nojiri, Phys. Rev. Lett. **92**, 031303 (2004) [arXiv:hep-ph/0307216].
  - [15] S. Profumo, Phys. Rev. **D72**, 103521 (2005). [astro-ph/0508628].
  - [16] J. March-Russell, S. M. West, D. Cumberbatch and D. Hooper, JHEP **0807**, 058 (2008) [arXiv:0801.3440 [hep-ph]].

- [17] N. Arkani-Hamed, D. P. Finkbeiner, T. R. Slatyer and N. Weiner, Phys. Rev. D **79**, 015014 (2009) [arXiv:0810.0713 [hep-ph]].
- [18] Q. Yuan, X. -J. Bi, J. Liu *et al.*, JCAP **0912**, 011 (2009). [arXiv:0905.2736 [astro-ph.HE]].
- [19] M. Lattanzi and J. I. Silk, Phys. Rev. D **79**, 083523 (2009) [arXiv:0812.0360 [astro-ph]].
- [20] R. Iengo, JHEP **0905**, 024 (2009) [arXiv:0902.0688 [hep-ph]].
- [21] R. Iengo, arXiv:0903.0317 [hep-ph].
- [22] J. L. Feng, M. Kaplinghat and H. B. Yu, Phys. Rev. Lett. **104**, 151301 (2010) [arXiv:0911.0422 [hep-ph]].
- [23] J. L. Feng, M. Kaplinghat and H. B. Yu, arXiv:1005.4678 [hep-ph].
- [24] E. Komatsu *et al.*, arXiv:1001.4538 [astro-ph.CO].
- [25] O. Adriani *et al.*, Phys. Rev. Lett. **102**, 051101 (2009) [arXiv:0810.4994 [astro-ph]].
- [26] O. Adriani *et al.* [PAMELA Collaboration], “PAMELA results on the cosmic-ray antiproton flux from 60 MeV to 180 GeV in kinetic energy,” arXiv:1007.0821 [astro-ph.HE].
- [27] A. A. Abdo *et al.* [The Fermi LAT Collaboration], Phys. Rev. Lett. **102**, 181101 (2009) [arXiv:0905.0025 [astro-ph.HE]].
- [28] M. Ackermann *et al.* [The Fermi-LAT collaboration], “Fermi LAT observations of cosmic-ray electrons from 7 GeV to 1 TeV,” arXiv:1008.3999 [astro-ph.HE].
- [29] J. J. Engelmann, P. Ferrando, A. Soutoul, P. Goret and E. Juliusson, Astron. Astrophys. **233**, 96 (1990).
- [30] A. D. Panov *et al.*, arXiv:0707.4415 [astro-ph].
- [31] H. S. Ahn *et al.*, Astropart. Phys. **30**, 133 (2008) [arXiv:0808.1718 [astro-ph]].
- [32] A. A. Abdo *et al.* [The Fermi-LAT collaboration], Phys. Rev. Lett. **104**, 101101 (2010) [arXiv:1002.3603 [astro-ph.HE]].
- [33] S. Cassel, arXiv:0903.5307 [hep-ph].
- [34] T. R. Slatyer, JCAP **1002**, 028 (2010) [arXiv:0910.5713 [hep-ph]].
- [35] J. Hisano, S. Matsumoto, M. Nagai, O. Saito and M. Senami, Phys. Lett. B **646**, 34 (2007) [arXiv:hep-ph/0610249].
- [36] X. l. Chen, M. Kamionkowski and X. m. Zhang, Phys. Rev. D **64**, 021302 (2001) [arXiv:astro-ph/0103452].
- [37] S. Hofmann, D. J. Schwarz and H. Stoecker, Phys. Rev. D **64**, 083507 (2001) [arXiv:astro-ph/0104173]

- [38] T. Bringmann and S. Hofmann, JCAP **0407**, 016 (2007) [arXiv:hep-ph/0612238].
- [39] J. B. Dent, S. Dutta and R. J. Scherrer, Phys. Lett. B **687**, 275 (2010) [arXiv:0909.4128 [astro-ph.CO]].
- [40] J. Zavala, M. Vogelsberger and S. D. M. White, Phys. Rev. D **81**, 083502 (2010) [arXiv:0910.5221 [astro-ph.CO]].
- [41] J. Hisano, S. Matsumoto, M. M. Nojiri and O. Saito, Phys. Rev. D **71**, 063528 (2005) [arXiv:hep-ph/0412403].
- [42] V. Barger, Y. Gao, W. Y. Keung, D. Marfatia and G. Shaughnessy, Phys. Lett. B **678**, 283 (2009) [arXiv:0904.2001 [hep-ph]].
- [43] S. Palomares-Ruiz and J. M. Siegal-Gaskins, JCAP **1007**, 023 (2010) [arXiv:1003.1142 [astro-ph.CO]].
- [44] N. Bernal and S. Palomares-Ruiz, arXiv:1006.0477 [astro-ph.HE].
- [45] M. Cirelli, P. Panci and P. D. Serpico, Nucl. Phys. B **840**, 284 (2010) [arXiv:0912.0663 [astro-ph.CO]].
- [46] R. C. Cotta, J. A. Conley, J. S. Gainer, J. L. Hewett and T. G. Rizzo, arXiv:1007.5520 [hep-ph].
- [47] I. Cholis and L. Goodenough, arXiv:1006.2089 [astro-ph.HE].
- [48] K. Ishiwata, S. Matsumoto and T. Moroi, arXiv:1008.3636 [hep-ph].
- [49] G. Belanger, F. Boudjema, A. Pukhov and A. Semenov, Comput. Phys. Commun. **180**, 747 (2009) [arXiv:0803.2360 [hep-ph]]; G. Belanger, F. Boudjema, A. Pukhov and A. Semenov, Comput. Phys. Commun. **176**, 367 (2007) [arXiv:hep-ph/0607059].
- [50] I. V. Moskalenko and A. W. Strong, Astrophys. J. **493**, 694 (1998) [arXiv:astro-ph/9710124].
- [51] A. W. Strong, I. V. Moskalenko and V. S. Ptuskin, Ann. Rev. Nucl. Part. Sci. **57**, 285 (2007) [arXiv:astro-ph/0701517].
- [52] J. N. Bahcall and R. M. Soneira, Astrophys. J. Suppl. **44**, 73 (1980).
- [53] J. F. Navarro, C. S. Frenk and S. D. M. White, Astrophys. J. **462**, 563 (1996) [arXiv:astro-ph/9508025].
- [54] J. F. Navarro *et al.*, arXiv:0810.1522 [astro-ph].
- [55] J. Diemand, *et al.* Mon. Not. Roy. Astron. Soc. **364**, 665 (2005) [arXiv:astro-ph/0504215].
- [56] A. A. Abdo *et al.* [The Fermi LAT Collaboration], Astrophys. J. **720**, 435 (2010) [arXiv:1003.0895 [astro-ph.CO]].

- [57] A. Abramowski *et al.* [H.E.S.S. Collaboration], Phys. Rev. Lett. **106**, 161301 (2011) [arXiv:1103.3266 [astro-ph.HE]].
- [58] P. Ciafaloni, D. Comelli, A. Riotto, F. Sala, A. Strumia and A. Urbano, arXiv:1009.0224 [hep-ph].
- [59] N. F. Bell, J. B. Dent, T. D. Jacques and T. J. Weiler, arXiv:1009.2584 [hep-ph].
- [60] S. Galli, F. Iocco, G. Bertone and A. Melchiorri, Phys. Rev. D **80**, 023505 (2009) [arXiv:0905.0003 [astro-ph.CO]].
- [61] T. R. Slatyer, N. Padmanabhan and D. P. Finkbeiner, Phys. Rev. D **80**, 043526 (2009) [arXiv:0906.1197 [astro-ph.CO]].
- [62] [Planck Collaboration], [astro-ph/0604069].